Journal of Thermal Analysis and Calorimetry, Vol. 78 (2004) 385–397

EFFECT OF HEATING RATE ON THE THERMAL PROPERTIES AND DEVOLATILISATION OF COAL

V. Strezov[1*], *J. A. Lucas*[2], *T. J. Evans*[3] *and L. Strezov*[2]

[1]Graduate School of the Environment, Macquarie University, NSW 2109, Australia
[2]The University of Newcastle, Department of Chemical Engineering, Callaghan, NSW 2308, Australia
[3]HIsmelt Corporation, Leath Rd, Kwinana, WA 6167, Australia

Abstract

The apparent specific heat of coal was measured by employing a computational calorimetric technique during continuous pyrolysis at heating rates of 10, 25 and 100°C min^{-1}. For all of the examined heating rates, the apparent specific heat was found to be approximately 1.4 kJ kg^{-1} K^{-1} at room temperature. When the sample reached decomposition temperature (~410°C), the specific heat increased to 1.9 kJ kg^{-1} K^{-1}. From this point, the apparent specific heat was greatly influenced by the coal reaction mechanism. For this purpose a detailed gas analysis was carried out for the three examined heating rates. It was found that with increased heating rates, the devolatilisation reactions were shifted to higher temperatures, as reflected in the measured apparent specific heat.

Keywords: coal, gas analysis, pyrolysis, specific heat, thermal analysis

Introduction

Coal is our major source of energy, and its utilisation will proceed with further developments of more sustainable and energy efficient technologies. Coal conversion comprises of combustion, gasification, pyrolysis and liquefaction, which essentially require thermal treatment under controlled process conditions, such as pressure, ambient atmosphere, coal type and heating rate. With the increased interest in hydrogen economy, coal will play major role as a source and carrier of hydrogen, and even further as an agent for steam reduction in the process of hydrogen generation. Furthermore, in the emerging direct ironmaking technologies, coal decomposition reactions play major role in reduction of metallic ores providing cleaner and environmentally sustainable smelting operation. In all of the coal conversion technologies coal decomposition is an intrinsic chemical reaction step in the utilisation process, and the effect of the process conditions to the decomposition reactions is of great importance for process optimisation and achieving increased energy efficiency. Heating rate, be-

* Author for correspondence: E-mail: vstrezov@gse.mq.edu.au

1388–6150/2004/ $ 20.00

Akadémiai Kiadó, Budapest
Kluwer Academic Publishers, Dordrecht

ing one of the parameters which affect the decomposition process including the release and composition of product volatiles, is a subject of study in the present work.

The macromolecular structure of coal consists of network of aromatic and hydroaromatic clusters crosslinked to each other by aliphatic or ether bridges [1]. When heating temperatures exceed 300°C, coal undergoes severe changes during which the bonds and bridges are broken, forming plastic phase. The plastic mass continues to decompose evolving primary gases and tars, which can further reform or decompose to secondary volatiles [2, 3]. Hydrogen evolution is generally occurring at temperatures greater than 500°C [4, 5] during which stronger carbon-hydrogen bonds are destroyed and an aromatic carbon rich structure reformed. Most of the hydrocarbons, however, are evolved during the plastic stage of decomposition in the temperature range of 400 and 600°C. Generally, bubbles of product volatiles are formed, competing with the surface viscous force of the plastic mass and resulting in bubble rupture and volatile release [6]. Heating rate has a clear effect on coal pyrolysis and evolution of volatile products, shifting the maximum rate of gas evolution to higher temperatures [7] and enhancing the plastic properties of the coals.

Coal thermal decomposition is essentially followed by consequent reactions, which have been extensively investigated using differential thermal analysis techniques [8–13]. Thermal properties are of great importance for both fundamental analysis of coal behaviour and for mathematical modelling of coal conversion processes. While the differential modes of thermal analysis, DSC and DTA, provide continuous observation of the thermal changes during reactions and decompositions, they have disadvantages in estimation of specific heats of materials. This is primarily due to the steady state heating requirements [14] during which large temperature intervals are applied in the measurements. Furthermore, very limited data is available in the open literature [15, 16] for an incorporated thermal and gas analysis measurements, which is required for classification of the thermal behaviour and better understanding of the coal decomposition reaction mechanism.

The recently developed Computer Aided Thermal Analysis technique [17] has the advantage of continuous measurement of the specific heat of materials with a potential for wide range of heating rate applications. This method was previously used for analysis of the major thermal regions of coal pyrolysis [6] where the thermal reactions were classified as dehydration, pre-plastic and plastic region, secondary devolatilisation and contraction of the carbon matrix. The current work investigates the effect of heating rate on coal thermal properties with incorporated gas analysis techniques for a comprehensive understanding of the coal decomposition mechanism.

Experimental

Sample

A coal sample with properties presented in Table 1 was selected for the analysis. The sample was ground to –212 μm and dried under vacuum at 80°C for 2 h to exclude the moisture content from coal. The sample selected for this study is from Australian origin and is a high volatile bituminous coal.

Table 1 Coal analysis

Proximate analysis				Ultimate analysis				
FC/%	VM/%	Ash/%	Moisture/%	C/%	H/%	N/%	O/%	S/%
55.8	32.2	9.2	2.8	84.1	5.16	1.92	8.18	0.64

Thermal property measurements

Specific heat of the coal sample was determined using Computer Aided Thermal Analysis technique. A detailed description of the experimental procedure can be found elsewhere [17]. Using range of calibration constants during the thermal property measurements, accuracy of approximately ±2% was achieved.

The thermal analysis apparatus is illustrated schematically in Fig. 1 and consists of an infrared furnace and an arrangement of internals for heating of a packed bed of sample. Coal powder with 2.3 g mass was packed in a silica glass tube to the density of 900 kg m^{-3}. The sample was insulated on the sides with ceramics and heated under argon atmosphere with a graphite heating element positioned inside the furnace. In this work, the heating rate of the furnace was fixed at 10, 25 and 100°C min^{-1} and the heating was carried out until the graphite temperature reached 1000°C. Temperatures of the graphite, surface and centre of the packed coal powder were acquired at a frequency of 1 Hz using chromel-alumel thermocouples.

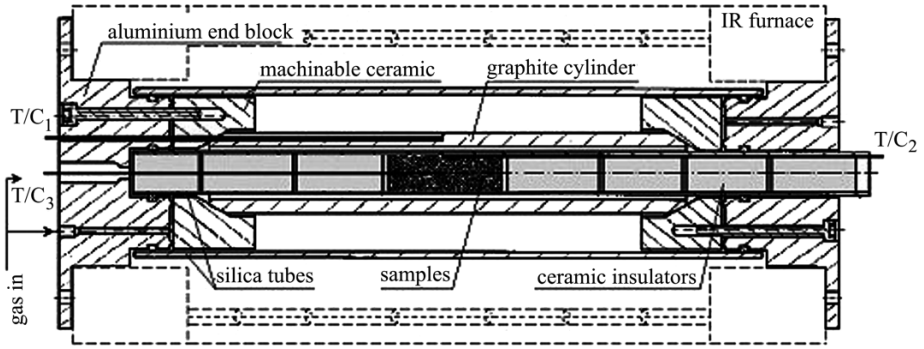

Fig. 1 Schematic diagram of the thermal analysis instrument

The specific heat was estimated simultaneously by applying an inverse numerical technique to the measured temperatures. In the calculations, the sample was divided into a grid pattern with a number of nodes (n) across the radius. The heat balance was calculated based on the principle where the heat accumulation by the node equals the difference of the heat entered and heat released from the node. The boundary conditions of the system were the temperatures measured at the centre and surface of the sample, zero heat flux in the centre of the sample and the surface heat flux calculated assuming radiative heat transfer from the graphite tube to the sample, as described by Eq. (1):

$$Q=F_{1-2}\sigma(T_g^4-T_s^4) \quad (1)$$

where Q – heat flux (W m^{-2}), F_{1-2} – radiation shape factor (–), σ – Stefan Boltzmann constant, T_g – graphite temperature (K), and T_s=sample temperature (K).

The radiation shape factor is a function of the emissivities of both the glass and graphite tubes, as well as their surface areas and was determined through calibration. To ensure uniform emissivity across the glass, the sample tube was coated with a thin layer of carbon soot.

The inverse numerical technique detailed in [18, 19] was implemented in an attempt to accurately determine the specific heat of the sample. This model was essentially derived from one dimensional heat conduction Eq. (2).

$$C_p\frac{\partial T}{\partial t}=\nu k\frac{\partial}{\partial r}\left(r\frac{\partial T}{\partial r}\right) \quad (2)$$

where ν – specific volume (m^3 kg^{-1}), C_p – specific heat (J kg^{-1} K^{-1}), k – thermal conductivity (W m^{-1} K^{-1}), T – temperature (K), t – time (s), r – radius (m).

As a result, Eq. (3) was derived and a computational matrix generated for an estimate of the specific heat. The specific heat estimated in this manner has apparent values, which means that the heats evolved during decomposition ΔH of the heated coal are included ($C_p=C_p^*+\Delta H/\Delta T$). Therefore, during an endothermic heat effect, the specific heat shows increase in the values, while during an exothermic reaction the specific heat values decrease. Reported results for the specific heat in the current work are generally based on the initial mass of the sample.

$$C_p=\frac{2\pi n\Delta x\nu Q_t}{\frac{\Delta x^2\pi}{4\Delta t}(T_0^t-T_0^{t-1})+\frac{\Delta x^2\pi}{\Delta t}\left(n-\frac{1}{4}\right)(T_n^t-T_n^{t-1})+\sum_{i=1}^{n-1}\frac{2\pi\Delta x^2 i}{\Delta t}(T_i^t-T_i^{t-1})} \quad (3)$$

It should be noted here that the experimental setup for this type of analysis simulates a fixed bed pyrolyser, which means that coal devolatilisation can be influenced by the size of coal particles and sample bed. Furthermore, coal carbonisation effect will certainly be emphasised in this arrangement, therefore the results presented by the thermophysical analysis depict the reaction mechanism and values for the current heating conditions and parameters.

Gas analysis

TG-FTIR method

The TG-FTIR instrument developed at Advanced Fuel Research was applied independently for analysis of the tars and seven volatile species (CH_4, C_2H_4, H_2O, CO, CO_2, NH_3 and HCN) during coal pyrolysis, from room temperature up to 1100°C, under the three different heating rates (10, 25 and 100°C min^{-1}). The instrument consists of a thermogravimetric analyser (TG) coupled with a Fourier-Transform Infra-

red (FTIR) spectrometer for the analysis of evolved volatiles. A detailed description of the technique can be found in the references [20, 21].

During these measurements, the sample is typically suspended from a balance in a gas stream within a furnace. The decomposing volatile products are carried out of the furnace into a gas cell, which is preheated at 115°C and where the volatiles are analysed by FT-IR spectroscopy. The rate of acquisition of the FT-IR spectra is at approximately each 30–40 s intervals. In the current experiments, helium carrier gas was passed through an oxygen trap with a flow of 310 mL min^{-1} through the TG system and a total gas flow through the cell of 848 mL min^{-1}. In the TG-FTIR runs, the initial sample mass was kept at around 40–50 mg.

Mass spectrometry

A Prima 600 mass spectrometer from VG Gas Analysis Systems was applied for analysis of hydrogen and H_2S, which were undetectable with the FTIR. The mass spectrometer was connected to the gas outlet of the furnace used for the thermal analysis with sample preparation, packing and experimental conditions identical as described above. The same heating rates were applied in the mass spectrometric study. The sample surface and centre thermocouples were disconnected during this part of analysis to avoid possible gas leaks from the thermocouple inputs. The graphite temperature was logged and used to calculate the temperature of the sample. Logging of the mass spectrometric data was done every 10 s.

Experimental results

Specific heat

Typical results of the specific heat during three consecutive measurements of the selected coal sample at a heating rate of 10°C min^{-1} are presented in Fig. 2. The results show good reproducibility with approximately ±2% of variations in the specific heat values, which corresponds to ±50 J kg^{-1} K^{-1}.

One of the results was selected and compared with the specific heat data for coals with similar rank found in the literature, as shown in Fig. 3. The comparison shows higher resolution of the current results where four measurements are produced for each degree Celsius, while the available literature results are in the order of one measurement every 25 to 50°C. Furthermore, there is very scarce data available in the literature for the coal specific heat in the temperature range where coal starts to decompose, therefore designers of coal conversion technologies are usually adopting the heat capacity model predictions. From the current results we can clearly observe that for temperatures below the plastic range, which for the studied coal was around 410°C, the specific heat data compares well with literature results. It was found that at room temperature the specific heat is 1370 J kg^{-1} K^{-1}, which corresponds well with the reported range of specific heats for dry coals of 1210 and 1470 J kg^{-1} K^{-1} [22]. At elevated temperatures the specific heat increased reaching 1880 J kg^{-1} K^{-1} at 410°C. There was a slight endothermic increase with a peak at 160°C due to the dehydration reaction. At temperatures exceeding 410°C, the

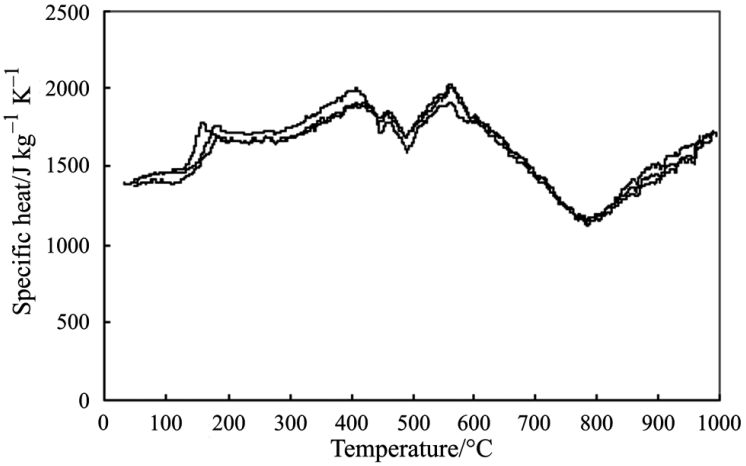

Fig. 2 Reproducibility of the specific heat data for three consecutive measurements, at a heating rate of 10°C min^{-1}

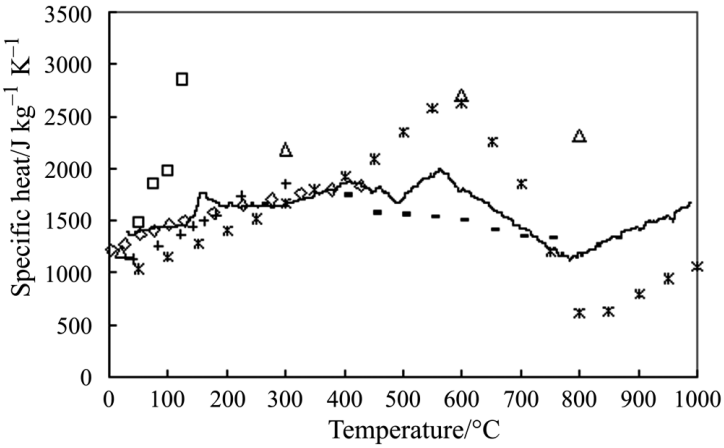

Fig. 3 Comparison of the specific heat from the current study determined at a heating rate of 10°C min^{-1} with published data for similar coals [15, 23–27]

apparent specific heat showed changes due to the decomposition reactions. The trend is generally similar to the published results exhibiting endothermic secondary reactions with a peak in the temperature range of 500 and 600°C followed by an exothermic contraction with a trough at 800°C.

There is an extensive range of models in the literature which can predict the specific heat of coal [22, 28–34], and have been summarised in Table 2. Apart from the models developed by Kirov [35] and Merrick [36], which have a theoretical approach, those presented in Table 2 are empirical, based on simple equation fitting to the experimental results, therefore, these models are limited to coals that have been

Table 2 Correlations for the specific heat of d.a.f. coal as a function of temperature T (K) or volatile matter VM (%) of the coal

Formulae for $C_{p\ d.a.f.}$ /J kg^{-1} K^{-1}	Temperature/°C	Author/Reference
$836.8 + 6.862VM–0.035VM^2$	15.5	Gomez [28]
$900+5VM$ $1155+24.7VM$	0 500	Kholler [29]
$716+1.5VM+0.44T$ (VM>14 mass%) $629+5.4VM+0.30T$ (VM<14 mass%)	<100	Clendenin *et al.* [30]
$849(1+0.008VM)(0.595+1.36\cdot10^{-3}T+6.752\cdot10^{-7}T^2–8.0\cdot10^{-10}T^3)$	<150	Fritz and Moser [30]
$443.5+1.036T+(11.862+7.1\cdot10^{-3}T)VM$	<1000	Lee [31]
$836.8+37.656\cdot10^{-3}(13+VM)(403+T)$	<250	Gladkov and Lebedev [32]
$1012.53(1+0.008VM)$	<100	Agroskin *et al.* [29]
$883\,(1+0.008VM)\left[1+0.0008\left(\frac{T-273}{100}\right)^3\right]$	<250	Agroskin *et al.* [29]
$–26.3+57.034\cdot10^{-3}T+9.808\cdot10^5T^{-2}$	50–175	Ordabaeva *et al.* [23]
$173.85+2.55T$	<350	Bliek *et al.* [33]
$95.685+2.155T$	<475	Weltner [32]
$[816+431(H/C+1.31O/C)][T–292.4]$	<350	Melchior and Luther [34]

analysed by the corresponding authors. For this reason, it is of larger interest to have applicable models to a variety of coals. In Kirov's model, for instance, a dry ash free coal was considered as a mixture of fixed carbon FC (coke), primary volatile matter (VM') and secondary volatile matter (VM''). The specific heat is then calculated as a sum of the specific heats of the coal constituents. Based on the Einstein quantum theory of the specific heat of solids, Merrick developed a model where the atoms of a d.a.f. coal are assumed to oscillate independently in three dimensions with two common characteristic frequencies. The specific heat is then calculated as a sum of the individual heat capacities. Figure 4 represents comparison of the specific heat data obtained in the current work with these model predictions. As the predictions are based on a dry-ash-free basis, results from the current work were also converted to d.a.f. values. It should be noted that Merrick's model predictions are preceded by a computational matrix which predicts devolatilisation of the major volatile products prior to calculation of the specific heat. Both models showed reasonably well predictions, especially at temperatures after completion of dehydration. At temperatures lower than 250°C, the specific heat was affected by the water content in the coal which is believed to be strongly bound, thereby current results showed values somewhat larger than the predictions. It appears that Kirov's model underpredicts the decomposition temperature, while Merrick's predictions corresponded well with the current results.

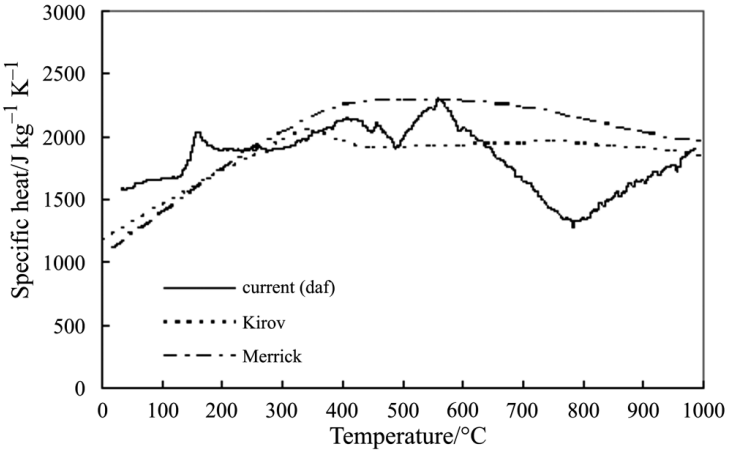

Fig. 4 Specific heat results compared with predictions from two models

Effects of heating rate

The major interest in the current study was to observe the effect of heating rate on the thermal properties and specific heat. For this purpose, the sample was subjected to thermal treatment under heating rates of 10, 25 and 100°C min^{-1}. Figure 5 presents the variations of the apparent specific heat with heating rate. For temperatures up to the decomposition point the specific heat showed similar values, apart from the endothermic release of the moisture. When the sample commenced its decomposition and consequent devolatilisation, the apparent specific heats were considerably different. The objective reason for these changes is in the reactions developed during thermal decomposition. The heating rates influenced the overall devolatilisation process affecting changes in the decomposition products.

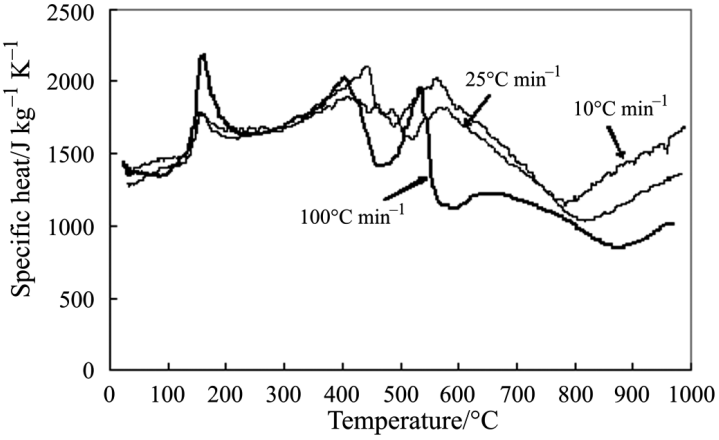

Fig. 5 Effect of heating rate on the apparent specific heat of coal

To clarify the effect of the volatile release on the apparent specific heat and thermal reactions, the sample was subjected to thermogravimetric and gas analysis techniques for the three examined heating rates. Table 3 gives synopsis of mass losses from balance readings and gas quantities from evolution and mass curves. The TG results in Fig. 6 show shift in the decomposition point towards higher temperatures with increased heating rate. Maximum rate of mass loss was found to extend from 480°C at 10°C min^{-1}, 495°C at 25°C min^{-1} to 520°C at the heating rate of 100°C min^{-1}. Figures 7–9 summarise the results from gas analysis measurements where a compari-

Table 3 Summary of TG-FTIR and Mass Spectrometric experiments (All yields are expressed in grams of a given product per gram of initial sample times 100% for the temperature of 900°C. Hydrogen and H_2S for the heating rate of 100°C min^{-1} were determined for the maximum temperature of 870°C)

Mass %	Heating rate /°C min^{-1}		
	10	25	100
Moisture	1.5	1.4	1.9
Ash	9.3	9.6	9.3
Tars	21.3	21.9	23.3
Tars (daf)	23.88	24.61	26.24
CH_4	2.90	2.7	2.7
CH_4 (daf)	3.25	3.03	3.04
C_2H_4	0.30	0.35	0.31
C_2H_4 (daf)	0.34	0.39	0.35
CO	3.50	3.10	2.30
CO (daf)	3.92	3.48	2.59
CO_2	1.10	1.10	1.00
CO_2 (daf)	1.23	1.24	1.13
H_2O	2.30	3.50	3.70
H_2O (daf)	2.58	3.93	4.17
H_2	0.78	0.81	0.40
H_2 (daf)	0.87	0.91	0.45
H_2S	0.07	0.01	0
H_2S (daf)	0.08	0.01	0
CS_2	0.04	0.04	0.03
CS_2 (daf)	0.04	0.04	0.03
HCN	0.17	0.14	0.12
HCN (daf)	0.19	0.16	0.14
NH_3	0.17	0.14	0.15
NH_3 (daf)	0.19	0.16	0.17

(daf) Dry Ash Free Basis

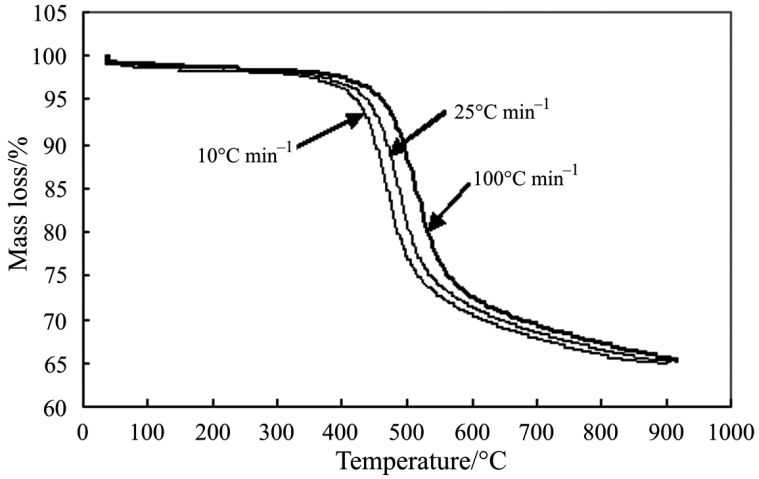

Fig. 6 TG curves of coal for three different heating rates

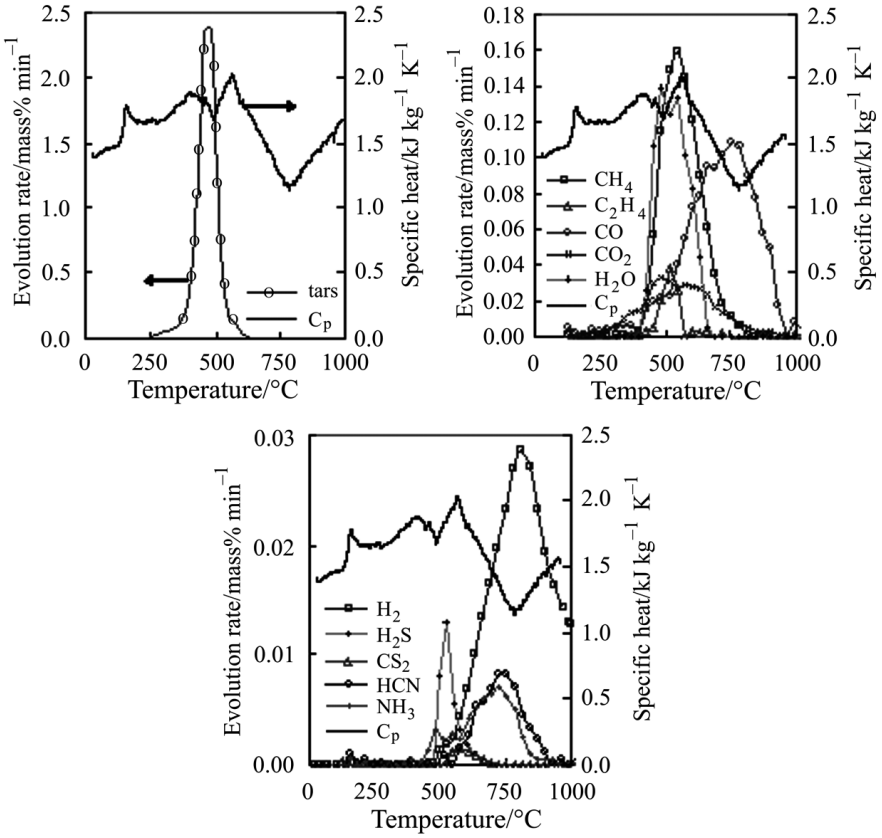

Fig. 7 Rate of evolution of tars and volatiles of coal heated at 10°C min^{-1}

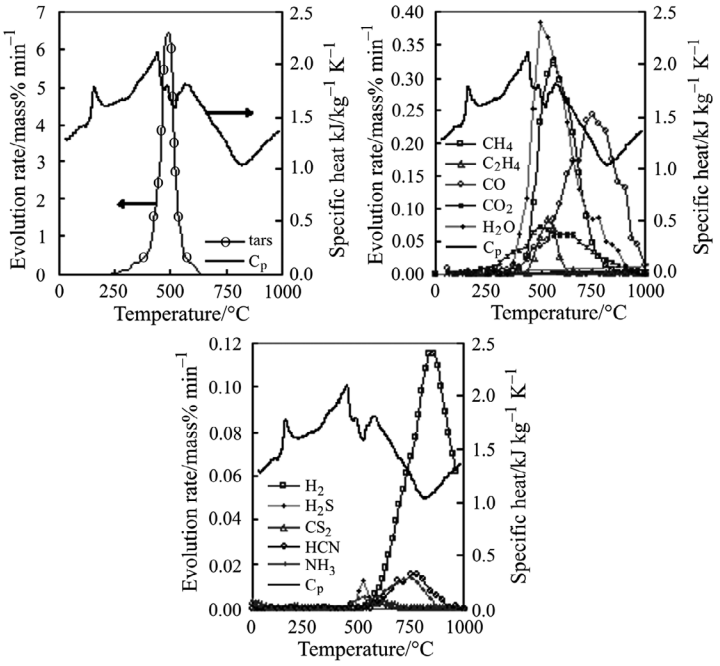

Fig. 8 Rate of evolution of tars and volatiles of coal heated at 25°C min^{-1}

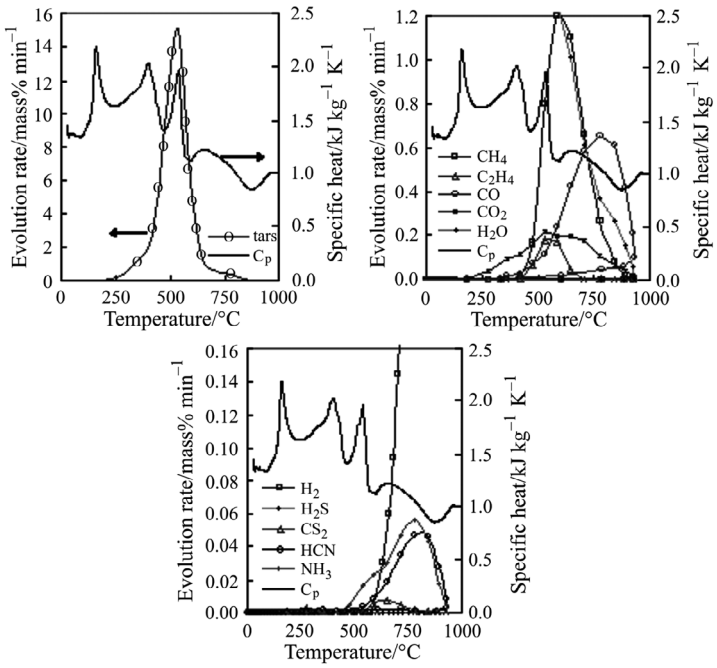

Fig. 9 Rate of evolution of tars and volatiles of coal heated at 100°C min^{-1}

son with apparent specific heat values from the thermal analysis is provided. The relationship between the evolution of tars and apparent specific heat indicates that the release of the same quantities of tars in a shorter period of time consumes larger energy for bond breaking and coincides with the endothermic heat release which was insignificant at 10°C min^{-1} and became stronger at higher heating rates.

The endothermic secondary reaction was the strongest at a heating rate of 10°C min^{-1} and appeared in the temperature range of 500 and 600°C. With increased heating rate, this reaction became very weak and occurred over wider temperature range. Most of the volatile constituents that evolved during this event were the hydrocarbons (CH_4 and C_2H_4), secondary water H_2O and CO_2, exhibitting peaks in the similar range as the endothermic heat release evident from the apparent specific heat data. Increased heating rates had similar effect on the exothermic contraction reaction, which was related to the evolution of hydrogen and had a trough extended from 780°C at 10°C min^{-1}, 820°C at 25°C min^{-1}, to 880°C at 100°C min^{-1}.

Conclusions

The apparent specific heat of coal was simultaneously determined at three different heating rates and compared with the consequent decomposition volatile products. The specific heat was approximately 1370 J kg^{-1} K^{-1} at room temperature and increased to 1880 J kg^{-1} K^{-1} at 410°C. After reaching decomposition temperature, the apparent specific heat was greatly influenced by the coal reaction mechanism. The endothermic reaction related to secondary devolatilisation was the strongest at the heating rate of 10°C min^{-1} and appeared in the temperatures between 500 and 600°C. The hydrocarbons, secondary water and CO_2 were the predominant volatiles which appeared in this range. At temperatures exceeding 600°C, the exothermic contraction reactions were detected with a trough extending from 780°C at 10°C min^{-1}, 820°C at 25°C min^{-1}, to 880°C at 100°C min^{-1}. Hydrogen was the dominant volatile released in this temperature range. The other volatiles, such as CO, HCN and NH_3 were also detected in the same region.

* * *

This program was funded by the Australian Research Council under the linkage project grant scheme (LP0454112). The TG-FTIR work was greatly assisted by the Advanced Fuel Research, CT and we are sincerely thankful to Dr. M. A. Wójtowicz and Ms R. Bassilakis for their contribution.

References

1 W. Wanzl, Fuel Process. Technol., 20 (1988) 317.
2 D. W. Van Krevelen, 'Coal Typology - Physics - Chemistry – Constitution', Elsevier Scientific Pub. Co., 1993.
3 M. A. Serio, D. G. Hamblen, J. R. Markham and P. R Solomon, Energy Fuels, 1 (1987) 138.
4 S. C. Saxena, Prog. Energy Combust. Sci., 16 (1990) 55.
5 V. Strezov, J. A. Lucas and L. Strezov, J. Anal. Appl. Pyrol., 71 (2004) 375.

6 J.-L. Yu, J. A. Lucas, V. Strezov and T. F. Wall, Energy Fuels, 17 (2003) 1160.
7 J. B. Howard, Chemistry of Coal Utilization, John Wiley & Sons, 1981 pp. 665–784.
8 R. J. Rosenvold, J. B. Dubow and K. Rajeshvar, Thermochim. Acta, 53 (1982) 321.
9 A. J. Lopez-Peinado, P. J. J. Tromp and J. A. Moulijn, Fuel, 68 (1989) 999.
10 S. K. Janikowski and V. I. Stenberg, Fuel, 68 (1989) 95.
11 O. P. Mahajan, A. Tomita and P. L. Walker, Jr, Fuel, 55 (1976) 63.
12 P. I. Gold, Thermochim. Acta, 42 (1980) 135.
13 J. P. Elder and M. B. Harris, Fuel, 63 (1984) 262.
14 J. Tomeczek and H. Palugniok, Fuel, 75 (1996) 1089.
15 X. Li, G. Matuschek, M. Herrera, H. Wang and A. Kettrup, J. Therm. Anal. Cal., 71 (2003) 601.
16 P. J. J. Tromp, F. Kapteijn and J. A. Moulijn, Fuel Process. Technol., 15 (1987) 45.
17 V. Strezov, J. A. Lucas and L. Strezov, J. Therm. Anal. Cal., 72 (2003) 907.
18 J. V. Beck, B. Blackwell and C. R. St Clair, Inverse Heat Conduction – Ill Posed Problems, John Wiley, New York 1985.
19 S. V. Patankar, Numerical Heat Transfer and Fluid Flow, Hemisphere Publishing Co., 1980.
20 R. M. Carangelo, P. R. Solomon and D. J. Gerson, Fuel, 66 (1987) 960.
21 J. K. Whelan, P. R. Solomon, G. V. Deshpande and R. M. Carangelo, Energy and Fuels, 2 (1988) 65.
22 M. V. Kök, J. Therm. Anal. Cal., 68 (2002) 1061.
23 A. T. Ordabaeva, B. T. Ermagambetov, B. K. Kasenov and E. S. Mustafin, Khimiya Tverdoga Topliva, 29 (1995) 35.
24 L. L. Isaacs and E. Tsafantakis, Prepr. Am. Chem. Soc. Div. Fuel Chem., 32 (1987) 243.
25 M. J. Richardson, Fuel, 72 (1985) 1047.
26 I. N. Nikolaev and N. I. Kozlova, Coke and Chemistry, 4 (1964) 7.
27 A. A. Agroskin, E. I. Goncharov, V. M. Tyangunov, I. G. Zubilin and V. B. Gleibman, Coke and Chemistry, 8 (1977) 14.
28 S. A. Newman, Hydrocarb. Process., 62 (1983) 77.
29 A. A. Agroskin and E. I. Goncharov, Coke and Chemistry, 7 (1965) 9.
30 F. Hanrot, D. Ablitzer, J. L. Houzelot and M. Dirand, Fuel, 73 (1994) 305.
31 A. L. Lee, Am. Chem. Soc. Div. Fuel Chem., 12 (1968) 19.
32 S. Badzioch, D. R. Gregory and M. A. Field, Fuel, 43 (1964) 267.
33 A. Bliek, W. M. van Poelje, W. P. M. van Swaaij and F. P. H. van Beckum, AIChE J., 31 (1985) 1666.
34 E. Melchior and H. Luther, Erdöl und Kohle, 28 (1975) 379.
35 N. Y. Kirov, BCURA Monthly Bulletin, 29 (1965) 33.
36 D. Merrick, Coal Science and Chemistry, Volborth, A. Ed., 1987 pp. 307–342.